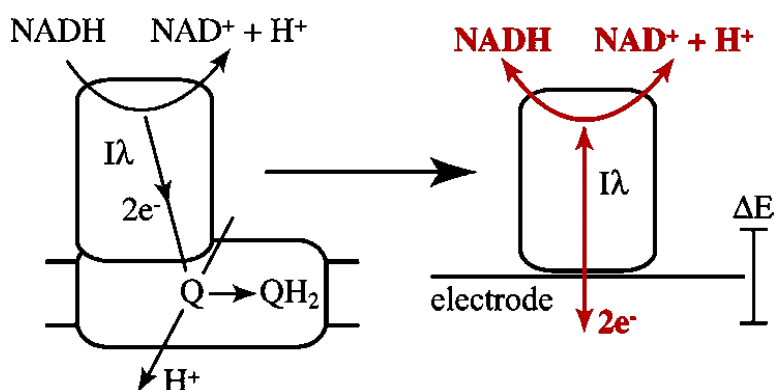


Reversible, Electrochemical Interconversion of NADH and NAD by the Catalytic (I λ) Subcomplex of Mitochondrial NADH:Ubiquinone Oxidoreductase (Complex I)

Yanbing Zu, Richard J. Shannon, and Judy Hirst

J. Am. Chem. Soc., **2003**, 125 (20), 6020-6021 • DOI: 10.1021/ja0343961 • Publication Date (Web): 30 April 2003

Downloaded from <http://pubs.acs.org> on March 26, 2009



More About This Article

Additional resources and features associated with this article are available within the HTML version:

- Supporting Information
- Links to the 6 articles that cite this article, as of the time of this article download
- Access to high resolution figures
- Links to articles and content related to this article
- Copyright permission to reproduce figures and/or text from this article

[View the Full Text HTML](#)



Reversible, Electrochemical Interconversion of NADH and NAD⁺ by the Catalytic (I_λ) Subcomplex of Mitochondrial NADH:Ubiquinone Oxidoreductase (Complex I)

Yanbing Zu, Richard J. Shannon, and Judy Hirst*

Medical Research Council Dunn Human Nutrition Unit, Hills Road, Cambridge, CB2 2XY, UK

Received January 29, 2003; E-mail: jh@mrc-dunn.cam.ac.uk

NADH:ubiquinone oxidoreductase (complex I) is the first enzyme of the respiratory electron transport chain.¹ It catalyses the oxidation of β-NADH by ubiquinone, coupled to transmembrane proton translocation. Complex I from bovine heart mitochondria is a membrane-bound assembly of probably 46 different proteins.² It contains a flavin mononucleotide (FMN) at the active site for NADH oxidation, up to eight iron–sulfur (FeS) clusters, and at least one ubiquinone binding site.³ The clusters transfer the electrons between NADH and ubiquinone, but their reduction and oxidation may also be coupled to proton transfer.⁴

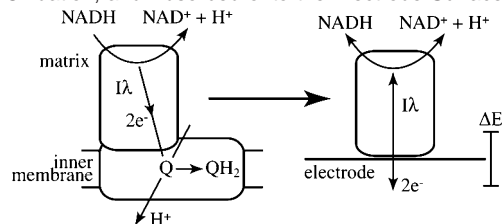
Complex I is L-shaped, with one arm in the membrane and the other protruding into the mitochondrial matrix.⁵ The extrinsic arm contains the FMN, the NADH binding site, and all of the FeS clusters and can be dissociated from bovine complex I to produce subcomplex I_λ.⁶ This communication describes the study of subcomplex I_λ by protein-film voltammetry.⁷ In addition to being the first report of reversible, electrocatalytic NADH/NAD⁺ interconversion, the catalytic behavior of subcomplex I_λ provides important new insights into the mechanism of complex I.

Subcomplex I_λ adsorbs onto the surface of a pyrolytic graphite edge electrode (Scheme 1), which it adopts as an electron acceptor or donor for the oxidation of NADH (high potentials) or the reduction of NAD⁺ (low potentials).⁸ Figure 1 shows how the current (the catalytic rate) responds to the applied potential (the thermodynamic driving force), as the potential is scanned continuously between two limits. Decreasing the scan rate does not influence the potential dependence of the catalytic current, which is therefore always at steady-state. Rotating the electrode maintains the surface concentrations of both NADH and NAD⁺ at their solution values. Therefore, the decrease in activity that occurs over consecutive cycles is not due to substrate depletion or product inhibition but is likely to be due to either enzyme instability or desorption. The decrease in activity may be exploited by measurement of the isosbestic points, formed where all the scans intersect.⁹ These denote the potential of zero net current (NADH oxidation balances NAD⁺ reduction), and therefore they occur at the reduction potential of NAD⁺, E_{NAD^+} .¹⁰

The continuous, sigmoidal waveshape of Figure 1 confirms that both NADH oxidation and NAD⁺ reduction are electrochemically reversible and do not require any overpotential. Considerable effort has been expended on developing an electrode surface capable of efficient and stoichiometric interconversion of NADH and NAD⁺, stimulated by the large number of NADH-coupled oxidoreductase enzymes that could then be exploited in biosensors and bioreactors.¹³ The directly coupled, adsorbed enzyme described here demonstrates, for the first time, selective and reversible bidirectional catalysis and provides a competitive alternative to small-molecule surface modifications.^{13,14}

The reversibility of the reaction is consistent with the match between the two-electron reduction potentials of the substrate and

Scheme 1. Subcomplex I_λ as a Part of Complex I, Catalyzing NADH Oxidation, and Adsorbed onto the Electrode Surface^a



^a During voltammetry, the catalysis is bidirectional, with the net direction imposed by the applied potential, ΔE .

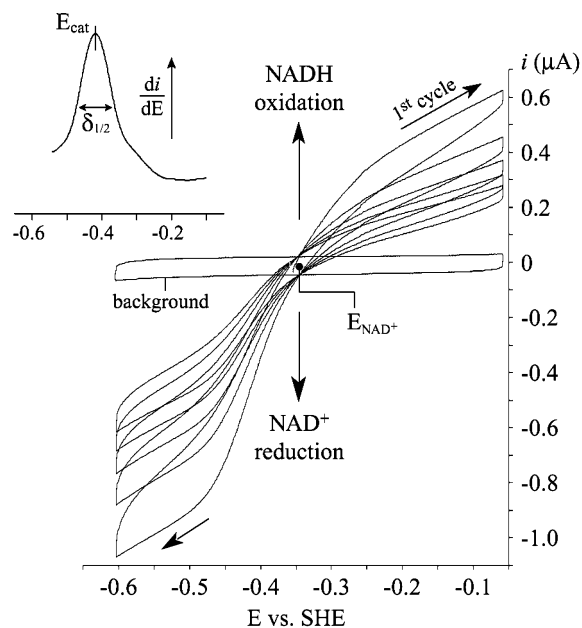


Figure 1. Reversible NADH oxidation and NAD⁺ reduction by subcomplex I_λ. The potential (driving force, *x*-axis) is cycled repeatedly, and the current (rate of catalysis, *y*-axis) is measured simultaneously. Catalytic currents are not affected by increasing the electrode rotation rate (mass-transport is not rate limiting) or by further increasing the substrate concentration (substrate binding is not rate limiting). The solution (pH 7.82) contained 1 mM NADH and 1 mM NAD⁺. Scan rate = 10 mV/s, rotation rate = 1000 rpm, 20 °C. The potential was prepoised for 10 s at the open circuit potential. Inset: the first derivative of the sum of scans 1–5, defining E_{cat} (the derivative maximum¹¹) and $\delta_{1/2}$ (the half-height width of the first-derivative peak; $\delta_{1/2} = 3.53RT/n_{\text{app}}F^{12}$). The origin of the shoulder at ca. -0.3 V is currently unknown.

the active site: at pH 7.8, E_{NAD^+} is -0.34 V (Figure 1) and E_{FMN} is -0.38 V.¹⁵ Because the semioxidized NAD[•] is very unstable,¹⁶ the catalytic reaction must be either a hydride transfer or a cooperative two-electron transfer.¹⁷ However, following its reaction with NADH (or NAD⁺), the flavin must be reoxidized (or

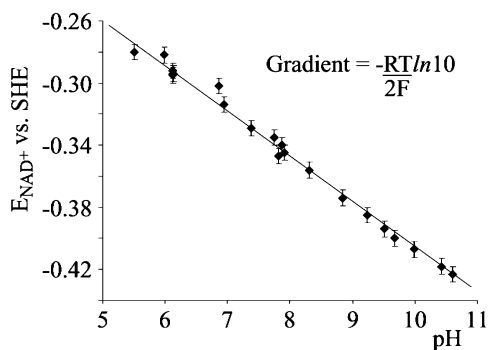
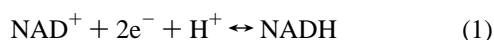


Figure 2. Isobestic points (E_{NAD^+}) as a function of pH, showing that catalysis remains reversible over a wide pH range. Conditions were the same as for Figure 1. The best fit line ($R^2 = 0.993$) has a gradient of -0.029 V/decade, as predicted for a $2e^-/1H^+$ couple. At low pH, values were recorded at higher ratios of NADH:NAD $^+$ (1:0.2), as NADH oxidation currents are small, and then extrapolated to 1:1 using the Nernst equation. Plots of reduction potential against $\ln([\text{NADH}]/[\text{NAD}^+])$ were linear.

rereduced) in two one-electron steps, by an iron–sulfur cluster. Analysis of the waveshape under conditions where the catalytic rate is not limited by mass transport (Figure 1) yields the apparent n -value, $n_{\text{app}} \approx 1$. Therefore, only one electron is transferred in the rate-limiting step, suggesting strongly that it is an electron-transfer event, not the substrate reaction between NADH and FMN. Similar behavior has been observed for several other flavoenzymes: succinate dehydrogenase,⁹ fumarate reductase,¹² and flavocytochrome c_3 .¹⁸ Figure 1 also shows that the catalytic waveshape is not ideal, since the current does not become potential independent at either limit. This is probably due to a distribution of the rates of interfacial electron transfer, which may become rate limiting at high overpotential and substrate concentration.¹⁹

At pH 7.82 (Figure 1), the negative currents from NAD $^+$ reduction achieve a larger magnitude (at $E \ll E_{\text{NAD}^+}$) than the positive currents from NADH oxidation (at $E \gg E_{\text{NAD}^+}$). Therefore, subcomplex I_L appears to be energetically biased in favor of NAD $^+$ reduction. From an electrochemical perspective, this is because the effective redox potential of the catalyst, E_{cat} , is more negative than the substrate potential.⁹ From the first derivative of the waveshape (Figure 1), E_{cat} is estimated to be -0.42 V at pH 7.82.¹¹ E_{cat} may include thermodynamic contributions from one or more of the ensemble of redox centers, as well as from pK values and binding constants, and it can be interpreted to identify the “control center” of the reaction. As discussed above, E_{cat} describes a one-electron transfer. At pH 7.8, E_{cat} is close to two known (one-electron) cofactor potentials in complex I:²⁰ FMN/FMN $\cdot H^+$ at -0.42 V¹⁵ and the potential of a [2Fe – 2S] cluster proximal to the FMN and the NADH binding site.²¹ This indicates that the rate-limiting step in NADH oxidation is either the second one-electron reoxidation of FMN $\cdot H_2$ or the oxidation or reduction of the proximal [2Fe – 2S] cluster.

Finally, the interconversion of NADH and NAD $^+$ (eq 1) requires proton transfer, and the reduction potential should therefore depend on pH, as given in the Nernst equation, eq 2.



$$E_{\text{NAD}^+} = E_{\text{NAD}^+}^{\circ} - \frac{RT}{2F} \left[\ln \frac{[\text{NADH}]}{[\text{NAD}^+]} + \text{pH} \ln 10 \right] \quad (2)$$

The pH dependence of E_{NAD^+} , measured from the isobestic points, is shown in Figure 2 and follows the theoretical prediction (eq 2). Therefore, catalysis remains reversible over a wide range of pH. Because the reduction potentials of the flavin and the [2Fe – 2S] cluster have different pH dependencies, determining how E_{cat} (relative to E_{NAD^+}) and the catalytic bias depend on pH will be crucial in identifying the exact source of E_{cat} . Investigations of how the catalytic waveshapes and potentials respond to variations in conditions (pH, ionic strength, and substrate concentrations) are expected to reveal further detailed information about how redox catalysis is controlled, and coupled to proton translocation, by complex I.

Acknowledgment. This work was supported by The Medical Research Council.

References

- (1) Saraste, M. *Science* **1999**, *283*, 1488–1493.
- (2) Carroll, J.; Shannon, R. J.; Fearnley, I. M.; Walker, J. E.; Hirst, J. *J. Biol. Chem.* **2002**, *277*, 50311–50317.
- (3) Walker, J. E. *Qu. Rev. Biophys.* **1992**, *25*, 253–324.
- (4) Hirst, J. *Proc. Natl. Acad. Sci. U.S.A.* **2003**, *100*, 773–775.
- (5) Grigorieff, N. *Curr. Opin. Struct. Biol.* **1999**, *9*, 476–483.
- (6) Preparation and characterization of subcomplex I_L have been described previously: Fearnley, I. M.; Carroll, J.; Shannon, R. J.; Runswick, M. J.; Walker, J. E.; Hirst, J. *J. Biol. Chem.* **2001**, *276*, 38345–38348.
- (7) Armstrong, F. A.; Heering, H. A.; Hirst, J. *Chem. Soc. Rev.* **1997**, *26*, 169–179.
- (8) Subcomplex I_L (30 μM) was applied to the surface of a freshly polished pyrolytic graphite edge rotating-disc electrode (diameter = 3 mm), which was then placed into solution in a thermostated all-glass electrochemical cell. pH was controlled by a mixed buffer system comprising 10 mM sodium acetate, MES, HEPES, and TAPS and checked immediately after each experiment. NaCl (0.1 M) was included as a supporting electrolyte. NADH and NAD $^+$ (Roche) were repurified prior to use (Orr, G. A.; Blanchard, J. S. *Anal. Biochem.* **1984**, *142*, 232–234). The counter electrode was a platinum wire, and a standard calomel reference electrode was used; all potentials have been corrected to the standard hydrogen electrode scale (Bard, A. J.; Faulkner, L. R. *Electrochemical Methods: Fundamentals and Applications*; Wiley: New York, 2001). Experiments were conducted in an anaerobic glovebox ($\text{O}_2 < 2$ ppm) using an Autolab Electrochemical Analyzer (EcoChemie) and an EG&G electrode rotator. No signals were observed in the absence of subcomplex I_L .
- (9) Hirst, J.; Sucheta, A.; Ackrell, B. A. C.; Armstrong, F. A. *J. Am. Chem. Soc.* **1996**, *118*, 5031–5038.
- (10) Clark, W. M. In *Oxidation–Reduction Potentials of Organic Systems*; Williams and Wilkins: Baltimore, 1960.
- (11) For an ideal waveshape, the potential of the maximum of the first derivative is equal to the midpoint potential of the catalytic wave. It is clear from Figure 1 that the current does not become potential independent at either high or low potential; thus, the midpoint potential cannot be defined. Only the derivative maximum has been used to define E_{cat} .
- (12) Heering, H. A.; Weiner, J. H.; Armstrong, F. A. *J. Am. Chem. Soc.* **1997**, *119*, 11628–11638.
- (13) Katakis, I.; Dominguez, E. *Mikrochim. Acta* **1997**, *126*, 11–32.
- (14) See, for example: Munteanu, F. D.; Mano, N.; Kuhn, A.; Gorton, L. *Bioelectrochem.* **2002**, *56*, 67–72. Bartlett, P. N.; Simon, E.; Toh, C. S. *Bioelectrochem.* **2002**, *56*, 117–122.
- (15) Sled, V. D.; Rudnitzky, N. I.; Hatfield, Y.; Ohnishi, T. *Biochemistry* **1994**, *33*, 10069–10075.
- (16) Farrington, J. A.; Land, E. J.; Swallow, A. J. *Biochim. Biophys. Acta* **1980**, *590*, 273–276.
- (17) Page, C. C.; Moser, C. C.; Chen, X.; Dutton, P. L. *Nature* **1999**, *402*, 47–52.
- (18) Butt, J. N.; Thornton, J.; Richardson, D. J.; Dobbin, P. S. *Biophys. J.* **2000**, *78*, 994–1009.
- (19) Léger, C.; Jones, A. K.; Albracht, S. P. J.; Armstrong, F. A. *J. Phys. Chem. B* **2002**, *106*, 13058–13063.
- (20) Ingledew, W. J.; Ohnishi, T. *Biochem. J.* **1980**, *186*, 111–117. Ohnishi, T. *Biochim. Biophys. Acta* **1998**, *1364*, 186–206.
- (21) The potential of the [2Fe – 2S] cluster in the overexpressed 24 kDa subunit is strongly dependent on conditions and covers a range from -0.41 to -0.49 V at pH 7.8 as the ionic-strength is varied (see: Zu, Y.; Di Bernardo, S.; Yagi, T.; Hirst, J. *Biochemistry* **2002**, *41*, 10056–10069). EPR measurements have previously reported a midpoint potential of -0.370 V at pH 7 in the intact mitochondrial enzyme and also that this cluster has a pH-dependent reduction potential (see ref 20).

JA0343961